International Immunopharmacology 73 (2019) 461–470

Contents lists available at ScienceDirect

International Immunopharmacology

journal homepage: www.elsevier.com/locate/intimp

Multitarget-based cotreatment with cilostazol and celecoxib synergistically suppresses collagen-induced arthritis in mice by enhancing interleukin-10 expression

So Youn Park[a,c,1], Yi Sle Lee[a,c,1], Sang Yeob Lee[b,1], Sung Won Lee[b], Ki Whan Hong[a], Chi Dae Kim[a,c,d,*]

[a] Gene & Cell Therapy Research Center for Vessel-associated Diseases, Pusan National University, Yangsan-si, Gyeongsangnam-do 50612, Republic of Korea
[b] Department of Internal Medicine, College of Medicine, Dong-A University, Busan 49202, Republic of Korea
[c] Department of Pharmacology, School of Medicine, Pusan National University, Yangsan-si, Gyeongsangnam-do 50612, Republic of Korea
[d] Research Institute for Convergence of Biomedical Science and Technology, Pusan National University Yangsan Hospital, Gyeongnam 50612, Republic of Korea

ARTICLE INFO

Keywords:
Cilostazol
Celecoxib
Rheumatoid arthritis
RANKL
NFATc1
TRAP

ABSTRACT

Cilostazol exerts potent anti-inflammatory effects and celecoxib, a COX-2 specific inhibitor, improves the unsatisfactory profile of NSAIDs. It was aimed to assess the anti-arthritic potential of celecoxib add-on for cilostazol therapy in collagen induced arthritis (CIA), and to elucidate the implication of interleukin (IL)-10 in the action of cilostazol and celecoxib cotreatment. Cotreatment of RAW 264.7 cells with 10 μM cilostazol and 0.3 μM celecoxib synergistically suppressed RANKL-induced increases in RANK mRNA and protein levels. When cultured in the presence of RANKL for 5 days, RANKL-stimulated expressions of osteoclastogenic genes (OSCAR, DC-STAMP, and cathepsin K mRNA) and the expression of RANK mRNA were markedly elevated. Furthermore, these gene expressions, including that of RANK, were significantly suppressed by cotreatment with cilostazol (10 μM) and celecoxib (0.3 μM). In addition, this co-treatment strongly down-regulated RANKL-induced NFATc1 protein and TRAP activity (key osteoclastogenic factors), and these down-regulations were significantly prevented by pretreating cells with IL-10 neutralizing antibody. Furthermore, increased osteoclast formation and extensive resorption pit formation by bone marrow-derived monocytes obtained from C57BL/6 mice cultured in the presence of M-CSF/RANKL were markedly suppressed by cilostazol and celecoxib cotreatment. Consequently, hindlimb paw thicknesses in DBA/1J CIA mice were significantly reduced by cilostazol (10 mg/kg/d) and celecoxib (5 mg/kg/d) cotreatment. These results were accompanied by synergistic suppression of cartilage depletion and bone erosion and reductions in arthritis scores in the CIA mice. In conclusion, serum IL-10 levels in these mice were markedly increased by cilostazol and celecoxib cotreatment, whereas elevated serum IL-1β levels were markedly reduced. Cotreatment with low-dose cilostazol and celecoxib may ensure the synergistic anti-arthritic potential.

1. Introduction

Rheumatoid arthritis (RA) is a systemic autoimmune disease characterized by systemic inflammation and multiple arthritis. In addition to synovial lesions, bones at inflamed joints of RA patients are destroyed by activated osteoclasts, which leads to deformity, disability, and severe pain [1]. Proinflammatory cytokines (e.g., IL-1β, IL-6, and TNF-α secreted by activated T cells play crucial roles in the pathogenesis of RA [2,3]. These cytokines stimulate synovial fibroblasts to produce RANKL, which subsequently induces osteoclasts to cause destruction of cartilage and bone [4].

RANKL, a member of the TNF family, plays important roles in

Abbreviations: BMM, bone marrow-derived macrophage-like cells; COX, Cyclooxygenase; DC-STAMP, Dendritic cell-specific transmembrane protein; M-CSF, Macrophage colony-stimulating factor; NFATc1, Nuclear factor of activated T cells cytoplasmic1; OSCAR, osteoclast-associated receptor; RANK, receptor activator of nuclear factor kB; RANKL, Receptor activator of NF-κB ligand; RA, Rheumatoid arthritis; SFs, Synovial fibroblasts; TRAP, Tartrate-resistant acid phosphatase

* Corresponding author at: Gene & Cell Therapy Research Center for Vessel-associated Diseases, Pusan National University, Yangsan-si, Gyeongsangnam-do 50612, Republic of Korea.
E-mail address: chidkim@pusan.ac.kr (C.D. Kim).
[1] These authors equally contributed to this work.

https://doi.org/10.1016/j.intimp.2019.05.058
Received 19 March 2019; Received in revised form 16 May 2019; Accepted 28 May 2019
Available online 03 June 2019
1567-5769/ © 2019 Elsevier B.V. All rights reserved.

osteoclast differentiation and activation [5,6]. Osteoclast precursor cells derived from hematopoietic cells undergo differentiation to tartrate-resistant acid phosphatase (TRAP)-positive mononuclear cells in the presence of macrophage colony stimulating factor (M-CSF) and receptor activator of NF-κB ligand (RANKL), and then fuse to form multinucleated cells that resorb bone matrix [7,8]. Inflammatory cytokines and cyclooxygenase (COX)-2 that are released from rheumatoid arthritis synovial fibroblasts (RASFs) are crucially involved in the destruction of articular bone and cartilage [9]. Furthermore, RANKL-induced activation of RANK receptor on the surfaces of osteoclast progenitor cells leads to the activation of nuclear factor of activated T cells cytoplasmic1 (NFATc1) that results in the differentiation of osteoclast progenitor cells into pathological cells that finally fuse to form multinucleated osteoclasts [7,8].

When activated, RASFs play a key role in the pathogenesis of RA synovitis through pannus formation. The inflammatory cytokines, matrix metalloproteinases (MMPs), and cyclooxygenase (COX)-2 are involved in the destruction of articular bone and cartilage [9,10]. As IL-1β and TNF-α induce RASF proliferation and stimulating the production of osteoclasts in association with RANKL, the downregulations of IL-1β, COX-2, and NFATc1 is viewed a major target of pharmaceutical therapy.

Cilostazol, an inhibitor of phosphodiesterase type III, suppresses proliferation of synovial fibroblasts from RA patients by enhancing apoptosis with increased cytochrome *c* release and apoptosis-inducing factor as well as increased caspase 3 activation via mediation of cAMP-dependent protein kinase activation-coupled Nrf2-linked increased HO-1 expression [11]. More interestingly, when BV-2 microglia were exposed to LPS, nitrite levels significantly increased in conjunction with the expressions of iNOS and COX2, and these increased variables were significantly attenuated by cilostazol (3–30 μM) [12]. Interestingly, Park et al. [13] reported cilostazol markedly elevated IL-10 levels in RA macrophage culture media and significantly reduced LPS-induced increases in TNF-α and IL-1β production. Celecoxib (COX-2 specific inhibitor) is a NSAID (non-steroidal anti-inflammatory drug) that selectively inhibits COX-2 and the production of PGE2 [14,15]. Celecoxib has also been reported to inhibit TNF-α-induced transcriptional activity and the DNA binding activity of NF-κB [16], and this negative regulation of NF-κB activation might importantly underlie its anti-inflammatory activity.

In the present study, we assessed the effects of cilostazol and celecoxib co-treatment on the up-regulation of serum IL-10 level, down-regulation of serum IL-1β and inhibition of the osteoclastogenic genes NFATc1 and TRAP expressions, thereby resulted in synergistic decrease in osteoclast formation and suppression of bone erosion in the CIA mouse under cotreatment with cilostazol and celecoxib.

2. Materials and methods

2.1. Animals

Male C57BL/6 mice (10 weeks of age) were purchased from Samtako Inc. (Osan, Gyunggi-do, South Korea), and male DBA/1J mice (8–12 weeks) from Japan SLC, Inc. (Shizuoka, Japan). All experimental procedures were conducted in accordance with the ethical and scientific procedures described in guidelines of the Pusan National University-Institutional Animal Care and Use Committee (PNU-IACUC). The mice were maintained under the conditions with a 12 h light-dark cycle at 22 °C and given ad libitum access to food and tap water in the Animal Research Center of Pusan National University.

2.2. Induction of collagen-induced arthritis (CIA) and treatment with cilostazol and celecoxib

Mice were immunized with 100 μg of bovine type II collagen (Chondrex, Redmond, WA) dissolved in 0.1 M acetic acid was emulsified with an equal volume of Freund's complete adjuvant (Sigma) intradermally at the tail base. 14 days after primary immunization, mice were boosted with bovine type II collagen supplemented with incomplete Freund's adjuvant in the same manner 14 days later. 10 mg/kg cilostazol or 5 mg/kg celecoxib was administered intraperitoneally beginning 3 days after the booster injection. Mice were euthanized on day 43, and knee joints were isolated.

Table 1
Severity scoring system in arthritis.

Clinical arthritis severity score	0	Normal
	1	Slight erythema or swelling
	2	Distinct erythematous swelling
	3	Joint distortion
	4	Ankylosis of the joint
Histological arthritis severity score	0	Normal
	1	Synovial inflammation - mild Synovial lesion - mild alteration Cartilage destruction - mild Bone erosion -mild
	2	Synovial inflammation - moderate Synovial lesion - moderate alteration Cartilage destruction - moderate Bone erosion - moderate
	3	Synovial inflammation - moderate Synovial lesion - severe destruction of the synovia Cartilage destruction – severe destruction with loss of cartilage Bone erosion - severe destruction, with disrupted joint architecture.

2.3. Assessments of histopathological arthritis

Arthritis severities in individual limbs were assessed by evaluating erythema, swelling, and other changes. Clinical arthritis and histological arthritis severities were scored, as previously described [17]. (Table 1).

2.4. Quantification of cytokine immunostaining in joint tissues

Tissue sections were obtained from paraffin blocks, rehydrated, and incubated with anti-RANK and anti-TNFα antibodies. Immunoreaction products were visualized using a broad-spectrum immunohistochemistry kit (Diaminobenzidine substrate kit, Vector Laboratories, Inc., Burlingame, CA).

2.5. Detection of osteoclasts and cartilage damage

Tissue sections were obtained from paraffin blocks, rehydrated, and stained with safranin-O for proteoglycan in articular cartilage and with tartrate-resistant acid phosphatase (TRAP) to detect osteoclasts. TRAP staining was performed using a TRACP staining kit (TaKaRa BIO INC.).

2.6. Culture of macrophages and bone marrow-derived cells

RAW264.7 macrophages were obtained from the American Type Culture Collection (Manassas, VA, U.S.A.) and cultured in RPMI containing 10% fetal bovine serum, 100 U/ml penicillin, and 100 μg/ml streptomycin at 37 °C in a humidified 5% CO2 air environment. Bone marrow cells were isolated from 10-week-old male C57BL/6 mice. Briefly, bone marrow cells harvested from femurs and tibiae were washed and layered on Histopaque-1077 (Sigma) and incubated in RPMI 1640 containing 10% FBS and M-CSF (25 ng/ml). After 24 h, culture dishes were washed to remove non-adherent cells, and adherent osteoclast precursor cells were incubated with M-CSF (25 ng/ml) and RANKL (100 ng/ml).

2.7. Western analysis

For Western blot analyses, cells were lysed in RIPA Lysis Buffer with cocktail of protease inhibitors (Sigma). Thirty μg of total protein from each sample was then loaded onto 10% SDS-polyacrylamide gels. Protein transferred to nitrocellulose membranes, which were immunoblotted with antibodies against RANK, NFATc1and β-actin. Protein bands were visualized using the Supersignal West Dura Chemiluminescent Substrate (Thermo Fisher Scientific Inc., Rockford, IL). Signals from bands were quantified using an UN-SCAN-IT gelTM software (Silk Scientific, Orem, UT).

2.8. RT-qPCR analysis

For measurement of gene expressions, total RNA isolation from cells using TRIzol reagent (Invitrogen, San Diego, CA) and RT-PCR were performed as previously described [18]. The mRNA levels were normalized to the human GAPDH. Data are analyzed using LightCycler 96 Software (Roche Molecular Biochemicals). Primer sequences are as follows:

GENE	Forward	Reverse
IL-10	CCA AGC CTT ATC GGA AAT GA	TCC TGA GGG TCT TCA GCT TC
TRAP(TRACP)	CAGCAGCCAAGGAGGACTAC	ACATAGCCCACACCGTTCTC
DC-STAMP	GTATCGGCTCATCTCCTCCA	AATCATGGACGACTCCTTGG
OSCAR	AATGGTCCTCATCTGCTTGG	CAAGGATCCCAGCTTCTCTG
Cathepsin K	CCAGTGGGAGCTATGGAAGA	AAGTGGTTCATGGCCAGTTC
RANK	GAAGATGCTTTGGTGGGTGT	TCAGTCGGGATCAGTGTGAG
GAPDH	ACCACGTCCATGCCATCAC	TCCACCACCCTGTTGCTGTA

2.9. Measurement of TRAP activity

RAW264.7 cells were fixed with 10% formaldehyde for 10 min and then with 95% ethanol for 1 min. Cells were incubated with 100 μl phosphatase substrate solution (3.7 mM *p*-nitrophenyl phosphate and 10 mM sodium tartrate in 50 mM citrate buffer, pH 4.6) at 37 °C for 30 min, and then the reaction was stopped with 100 μl of 0.1 N NaOH. Absorbance at 405 nm was measured using an ELISA reader.

2.10. Osteoclast formation

Murine osteoclasts were prepared from BMMs. In brief, bone marrow cells were cultured in RPMI 1640 containing 10% fetal bovine serum (FBS) and M-CSF (25 ng/ml) for 24 h. Nonadherent cells were harvested and cultured for 3 days in the presence of M-CSF (25 ng/ml). Floating cells were removed and adherent cells (bone marrow-derived macrophages; BMMs) were used as osteoclast precursors. To generate osteoclasts, BMMs were cultured with M-CSF (25 ng/ml) and RANKL (100 ng/ml) in the presence of cilostazol (10 μM) or celecoxib (0.3 μM) or cilostazol (10 μM) plus celecoxib (0.3 μM) for 14 days. Cultured cells were fixed and stained for TRAP using a TRACP staining kit (TaKaRa BIO INC.). Briefly, cultured BMMs were fixed using fixation solution for 5 min, washed, and incubated for 30 min at 37 °C with TRACP staining solution. TRAP-positive cells appeared dark red and TRAP-positive multinucleated cells containing more than three nuclei ($TRAP^+$ MNCs) were counted under an optical microscope (AXIO Imager. M2, ZEISS). TRAP-positive multinuclear cells ($TRAP^+$ MNCs) containing more than three nuclei were counted as osteoclasts.

2.11. Assessment of pit formation and actin ring staining

Osteoclast precursor cells obtained from the BMMs of C57BL/6 mice were incubated in a 96-well tissue culture plate with dentin slices (IDS, Boldon, UK). Cultures were maintained in RPMI 1640 containing 10% FBS, M-CSF (25 ng/ml), and RANKL (100 ng/ml) in the presence of cilostazol (10 μM) and/or celecoxib (0.3 μM) for 28 days. Culture media were replaced with fresh medium every 3 days. Pit formation images were obtained using a SUPRA40VP field emission scanning electron microscope (ZEISS).

For the actin ring formation assay, BMMs were treated with M-CSF (25 ng/ml) and RANKL (100 ng/ml) in the presence of cilostazol (10 μM) and/or celecoxib (0.3 μM) for 14 days. Cells were then washed in PBS and stained with a 50 μg/ml fluorescent phalloidin conjugate solution for 40 min. Images were obtained using a confocal microscope (LSM700, ZEISS).

2.12. Materials

Celecoxib and Cilostazol were purchased from Sigma-Aldrich (St. Louis, MO). Antibody specific for NFATc1 were purchased from Cell Signaling Technology (Beverly, MA). Antibodies specific for TNF-α and RNAK were purchased from Santa Cruz Biotechnology Inc. (Santa Cruz, CA). MCS-F and RANKL were purchased from Peprotech (Rocky Hill, NJ). IL-10 neutralizing antibody was purchased from R&D Systems (Minneapolis, MN).

2.13. Statistical analysis

Results were expressed as means ± SEMs. Concentration-dependent responses were analyzed using one-way analysis of variance followed by Tukey's multiple comparison tests. Statistical significance was accepted for $P < 0.05$.

3. Results

3.1. Synergistic inhibition of RANK expression by celecoxib and cilostazol cotreatment

RANKL plays an important role in osteoclast differentiation and activation [5,6]. RANKL receptor is expressed on the surfaces of pre-osteoclasts and plays an important role during osteoclastogenesis [19]. As shown in Fig. 1A and B, RANK mRNA and protein levels increased in a time-dependent manner when Raw 264.7 cells were incubated for 0, 6, 12 or 24 h with RANKL (100 ng/ml). RANK mRNA expression plateaued at 6 h, and RANK protein levels were significantly elevated at 12 and 24 h ($F_{3,11} = 19.93$, $P < 0.0005$). We also assessed whether cilostazol and celecoxib co-treatment suppressed the expression of RANK protein. After pretreatment with cilostazol (10 or 30 μM) and celecoxib (0.3–10 μM) for 4 h, Raw 264.7 cells were incubated with RANKL (100 ng/ml) for 24 h. The RANKL-induced RANK expression (2.27 ± 0.30-fold, $P < 0.05$) was significantly attenuated by cilostazol pretreatment at 30 μM to 1.22 ± 0.34-fold ($P < 0.05$), but not by cilostazol treatment at 10 μM (Fig. 1C). RANKL-induced RANK expression was also significantly suppressed by celecoxib at 1, 3, and 10 μM (each, $P < 0.05$) but not by celecoxib at 0.3 μM (Fig. 1D). Notably, 10 μM cilostazol and 0.3 μM celecoxib cotreatment (for 4 h) significantly reduced this RANKL-induced increase in RANK protein from 2.71 ± 0.20-fold to 0.95 ± 0.29-fold ($F_{5,17} = 8.133$, $P = 0.0015$), though either monotherapy with 10 μM cilostazol or 0.3 μM celecoxib showed no reduction (Fig. 1E). These results indicate cilostazol and celecoxib cotreatment dramatically and synergistically suppressed RANKL-induced RANK protein levels.

Further, upon exposure of RAW264.7 macrophages to RANKL (100 ng/ml) for 5 days, they showed an increased cell viability by 124.9 ± 4.6%. When cells treated with cilostazol (10 μM) or celecoxib (0.3 μM) alone and in combination for 4 h and then incubated for 5 days with RANKL (100 ng/ml), cell viability was not changed when compared with vehicle group (RANKL alone). These results indicate that the cilostazol and celecoxib did not inhibit the viability of RAW264.7 macrophages.

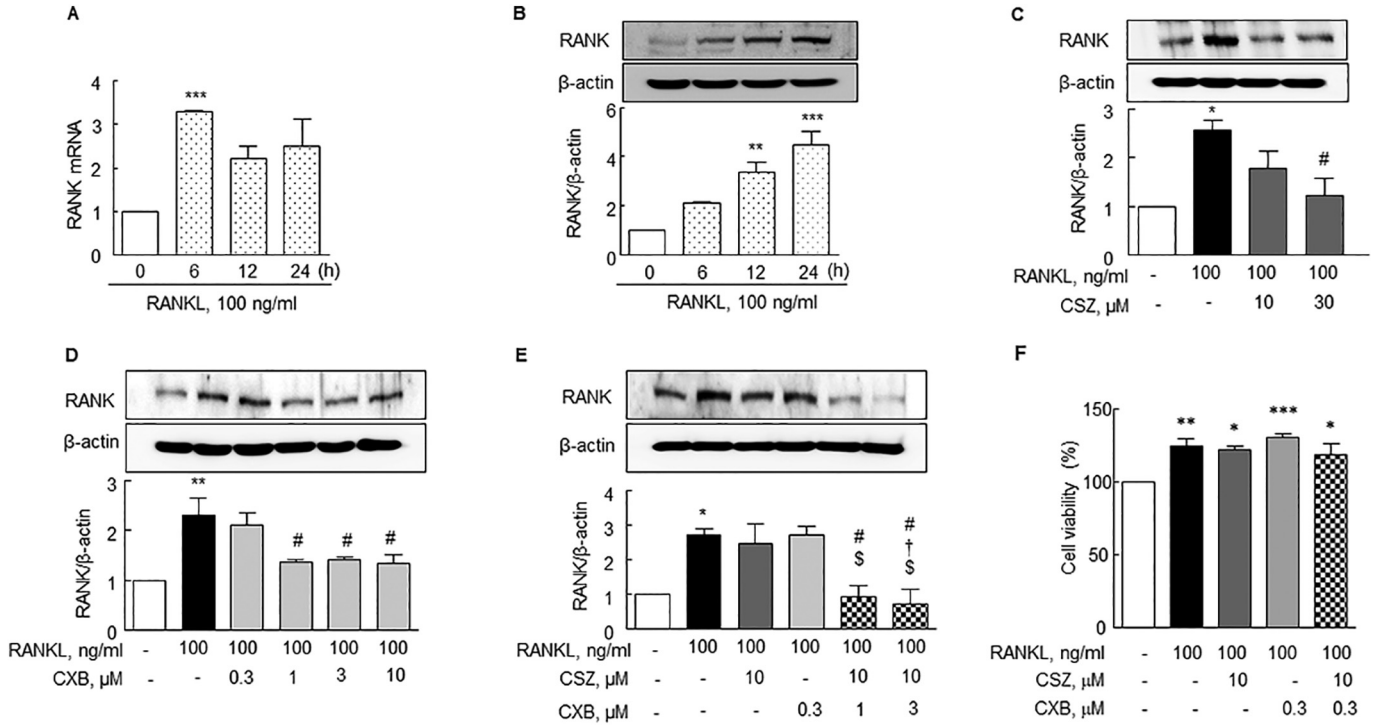

Fig. 1. Suppression of RANKL-induced RANK expression by cilostazol (CSZ) and celecoxib (CXB) in Raw 264.7 cells. (A, B) Time-dependent RANKL (100 ng/ml)-induced RANK mRNA and protein expressions. Cells were incubated for 0, 6, 12, or 24 h with RANKL (100 ng/ml). (C) Raw 264.7 cells were pretreated with CSZ (10 or 30 μM) for 4 h and then incubated for 24 h with RANKL (100 ng/ml). (D) Cells were pretreated with CXB (0.3, 1, 3, 10 μM) for 4 h and then incubated for 24 h with RANKL (100 ng/ml). (E) Cells were cotreated with CSZ (10 μM) and CXB (0.3, 1 μM) in comparison with effects by CSZ (10 μM) alone and CXB (0.3 μM) alone. (F) Viability of RAW264.7 macrophages after pretreatment with cilostazol (10 μM) or celecoxib (0.3 μM) with RANKL (100 ng/ml). The value for each group was calculated as the percentage of the none group (control = 100%). Results are expressed as the means ± SEMs of 4–5 independent experiments. $^{*}P < 0.05$, $^{**}P < 0.01$, $^{***}P < 0.001$ vs. non-treated controls; $^{\#}P < 0.05$ vs. RANKL (100 ng/ml) alone; $^{\dagger}P < 0.05$ vs. CSZ alone; $^{\$}P < 0.05$ vs. CXB alone.

3.2. Time-dependent RANKL-stimulated expressions of osteoclastogenic genes

Binding of RANKL to its receptor RANK activates multiple downstream signaling pathways that induce the expressions of key osteoclastogenic genes, such as those of osteoclast-associated receptor (OSCAR), dendritic cell-specific transmembrane protein (DC-STAMP), tartrate-resistant acid phosphatase (TRAP), and cathepsin K [7,8]. Raw 264.7 cells were pretreated with cilostazol (10 μM) plus celecoxib (0.3 μM) for 4 h and then incubated for 1 or 5 days with RANKL (100 ng/ml) to examine the effects of RANKL on the expression of osteoclastic genes OSCAR, DC-STAMP, and cathepsin K. After 1 day of RANKL treatment, the mRNAs of these genes were not expressed (Fig. 2Aa–d), but after 5 days, the expressions of three variables were markedly elevated as was that of RANK mRNA. These expressions were significantly suppressed by cilostazol (10 μM) alone but only marginally suppressed by celecoxib (0.3 μM) monotherapy. When cells were cotreated with celecoxib (0.3 μM) and cilostazol (10 μM), RANKL-stimulated expressions of OSCAR ($F_{4.14} = 342.2$, $P < 0.0001$), DC-STAMP ($F_{4.14} = 21.54$, $P < 0.0001$), cathepsin K mRNA ($F_{4.14} = 374.0$, $P < 0.0001$), and RANK mRNA were markedly suppressed ($F_{4.14} = 37.04$, $P < 0.0001$). Summarizing, cotreatment with cilostazol and celecoxib synergistically suppressed the up-regulations of OSCAR, DC-STAMP, cathepsin K, and RANK mRNAs by RANKL. It is considered that these decreases in the RANKL-induced osteoclastogenic gene expression by cilostazol and celecoxib are not ascribed to the cell death.

3.3. Synergistic inhibition of expressions of key osteoclastogenic genes NFATc1 and TRAP, and the suppression of osteoclast differentiation and pit formation

RANKL/RANK signaling activates downstream pathways, including those of NF-κB and NFATc1 [20], the latter of which is a master regulator of RANKL-induced osteoclast differentiation that induces the expression of TRAP, which is required for osteoclast differentiation. We examined effect of cilostazol (10 μM) and celecoxib (0.3 μM) cotreatment on the RANKL-stimulated NFATc1 protein expression and TRAP mRNA after 2 and 5 days, respectively, in cultured RAW 264.7 cells in the absence or presence of IL-10 neutralizing antibody pretreatment (NA, 2 μg/ml). As shown in Fig. 3A, RANKL (100 ng/ml) strongly stimulated NFATc1 expression to 3.24 ± 0.57-fold ($P < 0.01$). This increase was downregulated by pretreating cells with cilostazol (10 μM) and celecoxib (0.3 μM) by 1.64 ± 0.48-fold, and this down-regulation was reversed by pretreating cells with IL-10 neutralizing antibody (2 μg/ml) ($F_{5.23} = 8.991$, $P = 0.0002$).

In addition, RANKL-stimulated expression of TRAP mRNA increased to 261 ± 31.3-fold ($P < 0.001$), and this was reduced to 157.4 ± 11.9-fold ($P < 0.001$) by cilostazol pretreatment (10 μM), but not by celecoxib (0.3 μM). Interestingly, the RANKL-stimulated expression of TRAP mRNA was synergistically reduced to 49.1 ± 10.5-fold ($F_{4.14} = 86.01$, $P < 0.0001$) by cotreatment with cilostazol (10 μM) and celecoxib (0.3 μM) (Fig. 3B). Correspondingly, TRAP activity was increased by RANKL (100 ng/ml) by 1.57 ± 0.01-fold ($P < 0.001$), and this increase was significantly suppressed by cilostazol and celecoxib pretreatment to 1.05 ± 0.02-fold ($P < 0.01$). Furthermore, the suppression of TRAP activity by cilostazol and celecoxib was also prevented by pretreating with IL-10 neutralizing antibody (2 μg/ml) ($F_{5.23} = 22.43$, $P < 0.0001$) (Fig. 3C), indicating IL-10

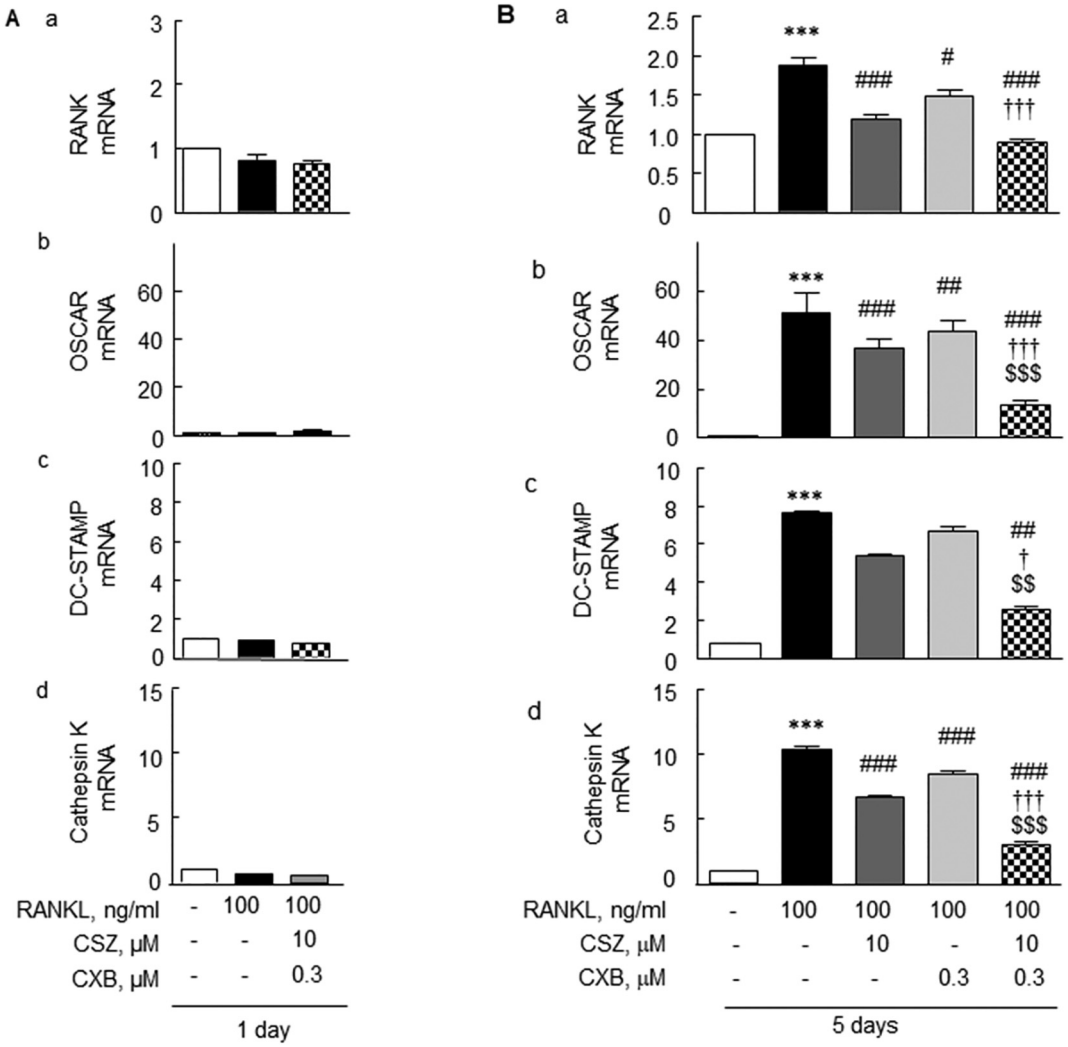

Fig. 2. Time-dependent RANKL-stimulated expressions of OSCAR, DC-STAMP, cathepsin K, RANK mRNA. (Aa–d) Raw 264.7 cells were cotreated with cilostazol (CSZ, 10 μM) plus celecoxib (CXB, 0.3 μM) for 4 h and then incubated for 1 day with RANKL (100 ng/ml). Results are expressed as the means ± SEMs of 4 experiments. (Ba–d) Comparison of effects of 10 μM CSZ and/or 0.3 μM CXB on the RANKL-induced expressions of OSCAR, DC-STAMP, cathepsin K, and RANK mRNA after incubation for 5 days. $^{***}P < 0.001$ vs. non-treated controls; $^{\#}P < 0.05$, $^{\#\#}P < 0.01$, $^{\#\#\#}P < 0.001$ vs. RANKL (100 ng/ml) alone. $^{\dagger}P < 0.05$, $^{\dagger\dagger\dagger}P < 0.001$ vs. CSZ alone; $^{\$\$}P < 0.01$, $^{\$\$\$}P < 0.001$ vs. CXB alone.

is involved in inhibition of NFATc1 and TRAP activity by cilostazol and celecoxib co-treatment.

Based on these results, we further examined whether osteoclast formation by BMDMs obtained from C57BL/6 mice cultured in the presence of M-CSF/RANKL was suppressed under cotreatment with cilostazol and celecoxib. In line with increased NFATc1 and TRAP expressions, M-CSF (25 ng/ml) plus RANKL (100 ng/ml) strikingly enhanced differentiation of BMDMs into multinucleated $TRAP^{+}$-giant cells (cells were incubated for 14 days) and this enhancement was slightly attenuated by the monotherapy with either cilostazol (10 μM) or celecoxib (0.3 μM). Interestingly, the enhanced osteoclast formation was strongly suppressed by cotreatment with cilostazol (10 μM) and celecoxib (0.3 μM) (Fig. 3D).

In addition, M-CSF (25 ng/ml) plus RANKL (100 ng/ml) caused actin ring formation, which is an indicative of osteoclast activity and bone resorption, suggesting that NFATc1- overexpressing osteoclast cells can resorb bone. These results showed that both size and number of actin ring structures were significantly reduced in a synergistical manner by cotreatment with cilostazol (10 μM) and celecoxib (0.3 μM). Both actin ring formation and extensive resorption pit formation observed for 28 days of incubation in the presence of RANKL (100 ng/ml) and M-CSF (25 ng/ml) on dentin slices were inhibited as evidenced by significantly reduced actin ring and bone resorbed areas of mature osteoclasts by cotreatment with cilostazol (10 μM) and celecoxib (0.3 μM) (Fig. 3E & F).

3.4. Suppression of the hindlimb paw thicknesses of CIA mice

In a previous study, we examined the suppression of paw edema by 20 mg/kg/d of cilostazol in a CIA mouse model [21]. Fig. 4A is showing representative features of macroscopic paw thickness of the hindlimb of DBA/1J CIA mice. In the CIA mice received vehicle, the hindlimb paw thickness was markedly increased with severe edema and redness when compared with sham mice. Hindlimb paw thickening was largely attenuated in the CIA mice treated with 10 mg/kg/d cilostazol and in less degree with 5 mg/kg/d celecoxib. Fig. 4B represents the measurement of paw thickness (in millimeters). Intriguingly, in CIA mice cotreated with 10 mg/kg/d cilostazol and 5 mg/kg/d celecoxib, paw thickening was much reduced at 43 days ($F_{4,19} = 74.67$, $p < 0.0001$). On the other hand, body weights in the study groups were similar (Fig. 4C).

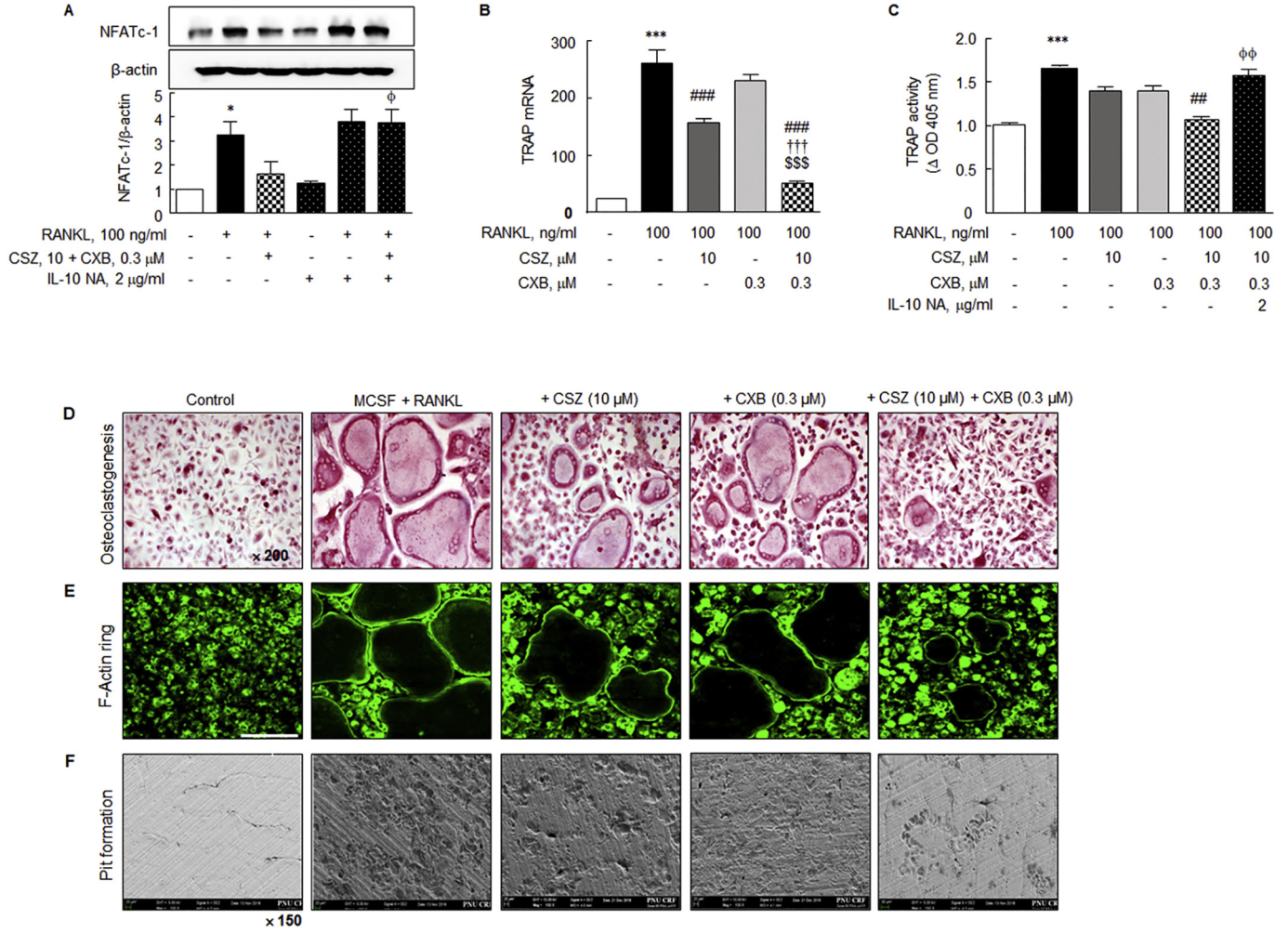

Fig. 3. (A) RANKL-stimulated expression of NFATc1 protein. Effects of 10 μM cilostazol (CSZ) and/or 0.3 μM celecoxib (CXB) on the RANKL-induced expressions of NFATc1 on day 2 in the absence or presence of 2 μg/ml of IL-10 neutralizing antibody (NA). Cells were pretreated with CSZ (10 μM) plus CXB (0.3 μM) for 4 h and then incubated for 2 days with RANKL (100 ng/ml). Results are expressed as the means ± SEMs of 4 experiments. (B) RANKL-stimulated TRAP mRNA expressions on day 5. (C) RANKL-stimulated TRAP activity in the absence or presence of 2 μg/ml of IL-10 neutralizing antibody (NA). Results are expressed as the means ± SEMs of 4 experiments. $^{**}P < 0.01$, $^{***}P < 0.001$ vs. non-treated controls; $^{\#\#}P < 0.01$, $^{\#\#\#}P < 0.001$ vs. RANKL alone. $^{\dagger\dagger\dagger}P < 0.001$ vs. CSZ alone; $^{\$\$\$}P < 0.001$ vs. CXB alone. $^{\phi\phi}P < 0.01$ vs. CSZ + CXB in the absence of IL-10 neutralizing antibody. In vitro morphological features of osteoclastogenesis were performed using TRAP staining (multinucleated TRAP^{+}-giant cells (D), F-actin ring (E), and pit formation (F) assays in BMDM cells treated with M-CSF (25 ng/ml) plus RANKL (100 ng/ml) with or without 10 μM of CSZ and/or 0.3 μM of CXB.

3.5. Suppressions of cartilage depletion, bone erosion and arthritis scores by cilostazol and celecoxib co-treatment

Blocks of 6 μm thickness were cut and stained with hematoxylin and eosin (H&E) for assessment of synovial inflammation and bone erosion and stained with safranin-O for proteoglycan in articular cartilage, and with TRAP for detection of osteoclasts. On day 43 after first injection, knee joints obtained from CIA mice showed structural alterations, which included thickened synovium with depleted proteoglycan and severe bone erosion as compared with sham controls. In addition, arthritis scores (markers of histological severity) of vehicle-treated CIA mice were significantly lower for cilostazol and celecoxib cotreated CIA mice (Fig. 5A). Furthermore, in CIA treated mice, joint spaces had been destroyed and large numbers of infiltrating inflammatory cells and pannus formation were observed, whereas joint spaces were well preserved in mice co-treated with cilostazol and celecoxib.

Safranin-O staining showed proteoglycan levels which were markedly reduced in vehicle-treated CIA mice, and that cilostazol and celecoxib co-treatment markedly reduced cartilage loss and preserved proteoglycan levels in knee joint cartilage. Furthermore, TRAP staining was extensive in vehicle-treated CIA mice, indicating considerable bone erosion, but was significantly less severe in mice cotreated with celecoxib and cilostazol.

In addition, we investigated the synergistic effects of cilostazol and celecoxib co-treatment on the progression of collagen-induced arthritis using arthritis scores, proteoglycan levels, and severities of bone erosion. As shown in Fig. 5B, cilostazol and celecoxib co-treatment significantly reduced mean arthritis score from 2.83 ± 0.17 in the vehicle group to 0.83 ± 0.31 ($F_{4,29} = 231.1$, $p < 0.0001$), mean proteoglycan thickness was depleted from 2.17 ± 0.11 (vehicle group) to 1.0 ± 0.36 ($F_{4,29} = 106.5$, $p < 0.0001$), and bone erosion 2.92 ± 0.08 (vehicle group) to 0.33 ± 0.21 ($F_{4,29} = 196.2$, $p < 0.0001$) in mice cotreated with celecoxib and cilostazol. On the other hand, cilostazol alone had only a slight effect and celecoxib alone had little effect. These results indicate cilostazol and celecoxib acted synergistically to reduce to severity of CIA.

3.6. Cotreatment with celecoxib and cilostazol increased anti-inflammatory cytokine production in CIA mice

RANKL-induced RANK expression in Raw 264.7 cells was synergistically and significantly reduced by cilostazol and celecoxib co-

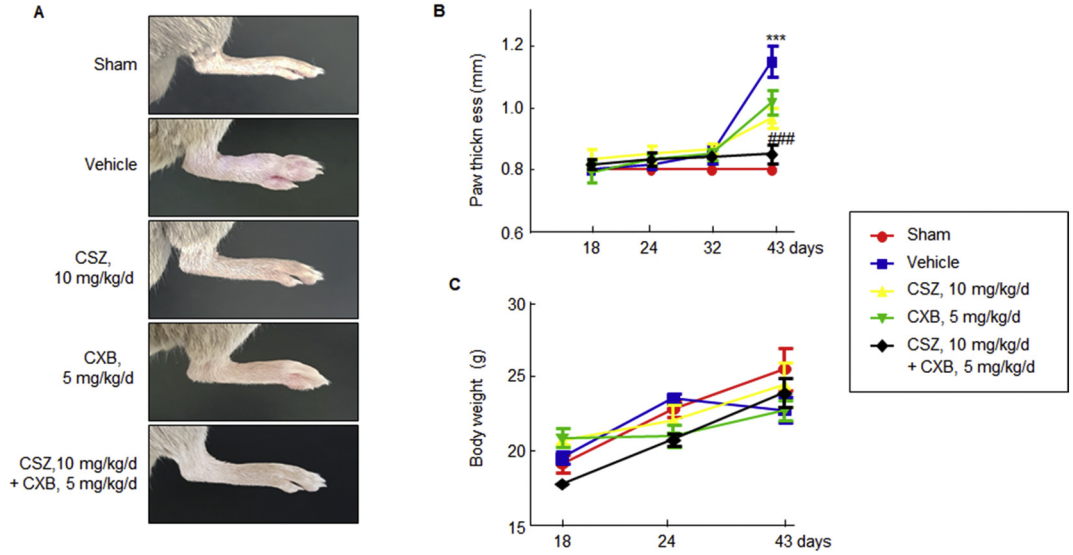

Fig. 4. (A) Representative macroscopic paw thickness features of the hindlimb of CIA mice. a, Sham DBA/1J mice; b, CIA + vehicle; c, CIA + cilostazol (CSZ) 10 mg/kg/d; d, CIA + celecoxib (CXB) 5 mg/kg/d; and e, CIA + CSZ 10 mg/kg/d + CXB 5 mg/kg/d treated mice. (B) Quantitative analyses: Paw thicknesses of CIA mice (shown in millimeters) were significantly reduced by cotreatment with cilostazol (10 mg/kg/d) plus celecoxib (5 mg/kg/d). Results are presented as the means ± SEM of 5 animals per group. $^{***}P < 0.001$ vs. Sham controls; $^{\#\#\#}P < 0.001$ vs. CIA/vehicle treated controls. (C) Changes in body weight.

treatment (at 10 and 0.3 μM, respectively). The immunohistochemical expressions of RANK and TNF-α in vehicle treated CIA mice were markedly greater than in sham controls, but strikingly attenuated by cilostazol and celecoxib co-treatment. On the other hand, cilostazol and celecoxib monotherapies had only marginal effects (Fig. 6A).

IL-10, an anti-inflammatory cytokine in rheumatoid synovium [22], was reported to be released by cilostazol into the culture media of RA macrophages, and LPS-induced increased TNF-α and IL-1β production was significantly reduced [13]. We identified the upregulation of IL-10 mRNA expression. As shown in Fig. 6Ba, Raw 264.7 cells were treated with cilostazol (10 μM) and celecoxib (0.3 μM) as a time course (0, 1, 3, 6, 12 and 24 h) effect on the expression of IL-10 mRNA. Cotreatment with cilostazol and celecoxib showed a maximum expression of IL-10 mRNA expression at 1 h and thereafter declined slowly ($F_{5.11} = 4.517$, $P = 0.0470$). When the monotherapy was compared with cotreatment (Fig. 6Bb), IL-10 mRNA expression was little affected by either cilostazol (10 μM) or celecoxib (0.3 μM) (treatment for 1 h), but cotreatment with cilostazol and celecoxib synergistically increased the IL-10 mRNA

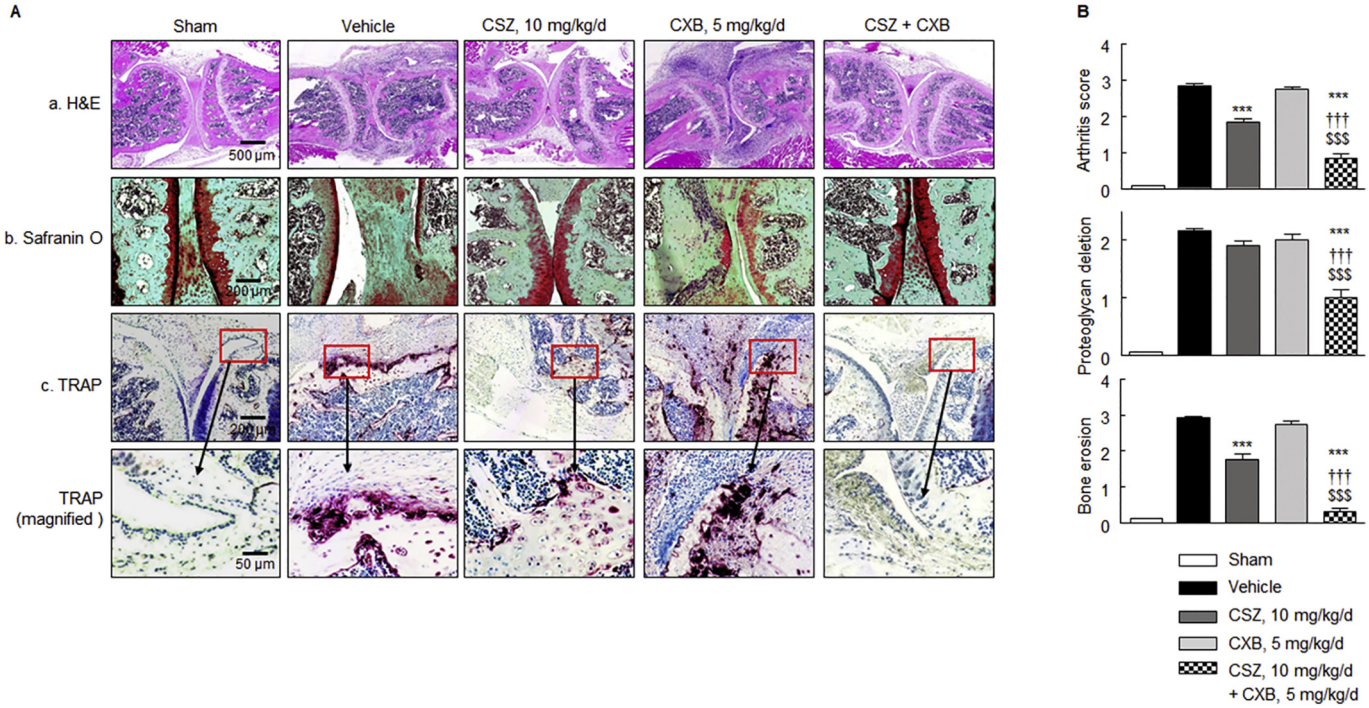

Fig. 5. Synergistic suppression of bone erosion by cilostazol and celecoxib co-treatment in mouse model of CIA. (A) Representative histological findings in knee joints (on day 43) from DBA/1J: hematoxylin-eosin (H&E), safranin-O, and TRAP-stained histological sections of knee joints (on day 43) of CIA mice treated with vehicle or 10 mg/kg/d of cilostazol (CSZ) and/or 5 mg/kg/d of celecoxib (CXB) and sections of sham controls. (B) Quantitative analyses: arthritis scores, proteoglycan deletion, and bone erosion scores of knee joints. Results are presented as the means ± SEM of six experiments. $^{***}P < 0.001$ vs. CIA/vehicle controls; $^{\dagger\dagger\dagger}P < 0.001$ vs. CIA/CSZ and $^{\$\$\$}P < 0.001$ vs. CIA/CXB treated mice.

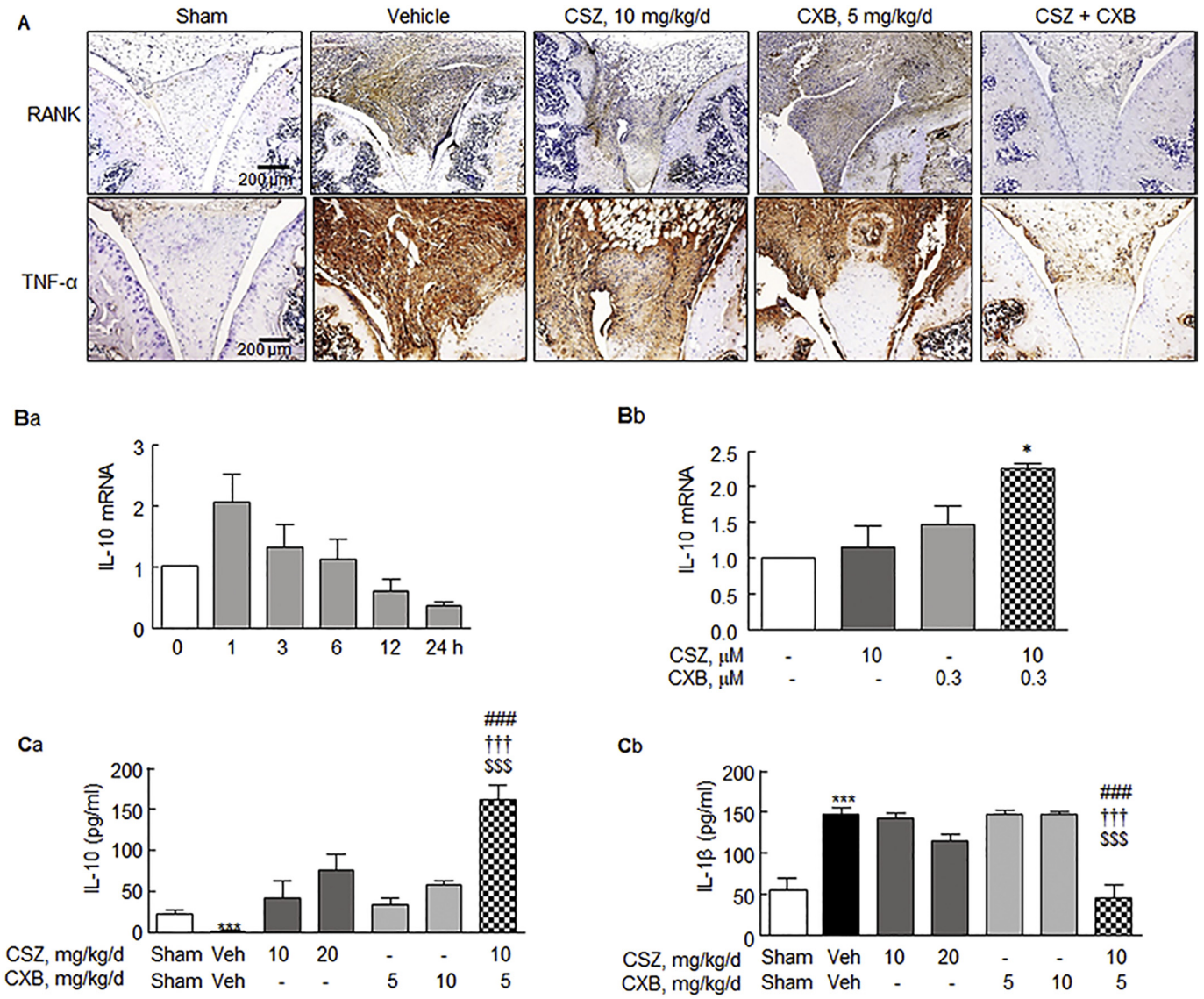

Fig. 6. (A) Representative histological sections of knee joints (on day 43) from DBA/1J sham and CIA mice treated with vehicle or 10 mg/kg/d of cilostazol (CSZ) and 5 mg/kg/d of celecoxib (CXB) alone and in combination, which were stained with RANK and TNF-α antibody. (Ba) Time course (0, 1, 3, 6, 12 and 24 h) effects on the expression of IL-10 mRNA in the Raw 264.7 cells after cotreatment with cilostazol (10 μM) and celecoxib (0.3 μM). (Bb) Synergistic increase in IL-10 mRNA expression by cotreatment with CSZ (10 μM) and CXB (0.3 μM) in the Raw 264.7 cells. $^{*}P < 0.05$ vs. None. (Ca, b) Significantly increased anti-inflammatory cytokine IL-10 level and decreased pro-inflammatory cytokine IL-1β production in the serum of CIA mice that cotreated with 10 mg/kg/d of cilostazol (CSZ) and 5 mg/kg/d of celecoxib (CXB), those of which were compared with the CSZ or CXB monotherapy. Results are presented as the means ± SEM of four experiments. $^{***}P < 0.001$ vs. Sham group mice; $^{\#\#\#}P < 0.001$ vs. Vehicle-administered CIA mice; $^{\dagger\dagger\dagger}P < 0.001$ vs. 10 mg/kg/d CSZ; $^{\$\$\$}P < 0.001$ vs 5 mg/kg/d CXB.

expression in Raw 264.7 cells ($F_{3,7} = 8.315$, $P = 0.0341$). In the CIA mice, serum IL-10 level from sham mice was 23.0 ± 8.86 pg/ml and that from vehicle group decreased to 0.69 ± 1.51 pg/ml ($P < 0.001$). Interestingly, serum IL-10 level from mice cotreated with cilostazol (10 mg/kg/d) and celecoxib (5 mg/kg/d) was strikingly increased to 161.38 ± 31.6 pg/ml, however, the CIA mice that received the monotherapy showed a marginal change ($F_{6,19} = 7.531$, $P = 0.0009$) (Fig. 6Ca).

Accordingly, serum IL-1β level from sham mice was 54.7 ± 18.4 pg/ml and that from vehicle-treated CIA mice was elevated to 146.3 ± 17.4 pg/ml ($P < 0.001$ vs. sham group). Serum IL-1β level from CIA mice cotreated with cilostazol (10 mg/kg/d) and celecoxib (5 mg/kg/d) was significantly decreased to 44.7 ± 34.7 pg/ml. Nevertheless, the serum level obtained from CIA mice that received each monotherapy revealed little difference from that of vehicle-treated CIA mice (Fig. 6Cb). These results indicate that upon cotreatment with celecoxib (5 mg/kg/d) and cilostazol (10 mg/kg/d), the anti-inflammatory IL-10 level synergistically increased and the pro-inflammatory IL-1β level synergistically decreased.

4. Discussion

The current study shows that cotreatment of Raw 264.7 cells with cilostazol and celecoxib synergistically suppresses RANKL-induced RANK expression and subsequently inhibits the expressions of osteoclastogenic genes, namely, OSCAR, DC-STAMP, cathepsin K and TRAP mRNA by up-regulating IL-10. Furthermore, cotreatment with cilostazol and celecoxib induced up-regulation of IL-10 and down-regulations IL-1β and TNF-α, consequently reduced osteoclast formation and bone resorption with reduced arthritis scores in a mouse model of CIA.

RANKL is known to bind specifically to RANK on osteoclast precursors, and that this interaction plays important roles during osteoclastogenesis in the presence of M-CSF [19]. Furthermore, the mechanisms of bone erosion and cartilage destruction in the CIA mouse

model have been shown to be dependent on RANKL/RANK signaling-induced osteoclast formation [23]. In the present study, RANK protein levels significantly increased in a time-dependent manner (between 12 and 24 h) when Raw 264.7 cells were stimulated with RANKL. However, cilostazol and celecoxib co-treatment significantly and synergistically attenuated RANKL-induced RANK expression, whereas either cilostazol or celecoxib monotherapy showed little effect.

RANKL is a key factor for differentiation of monocyte-macrophage lineage osteoclast precursors into multinucleated osteoclasts and for osteoclast maturation [19], and RANKL/RANK signaling stimulates several signaling pathways, including those of NF-κB, c-fos, and MAPKs [24,25], and these pathways activate NFATc1, a master regulator of osteoclast differentiation. NFATc1 regulates the expressions of genes encoding TRAP and cathepsin K [7] and is involved in osteoclast multinucleation by regulating the activity of DC-STAMP [26,27]. Park et al. [13] posited cilostazol suppressed LPS-stimulated increases in TLR4 expression by blocking the transcriptional activity of PU.1 in RA macrophages and found cilostazol down-regulated LPS-stimulated PU.1-linked TLR4 expression and TLR4/MyD88/NF-κB signal pathways and suppressed inflammatory cytokine production in synovial macrophages from RA patients. Interestingly, Funakoshi-Tago et al. [16] reported that celecoxib inhibited TNF-α-induced NF-κB activation by preventing the nuclear translocation of the p65 NF-κB subunit and supposed this inhibition of NF-κB activation contributed to its anti-inflammatory effects. Furthermore, as was reported by Takayanagi [28] involvements of OSCAR and RANK are required for osteoclast differentiation.

In the current study, RANKL-induced up-regulations of OSCAR, DC-STAMP and cathepsin K mRNA and RANK mRNA expression were markedly diminished by adding celecoxib at low concentration (0.3 μM) to cilostazol (10 μM). Furthermore, cilostazol and celecoxib co-treatment also diminished RANKL (100 ng/ml)-stimulated NFATc1, and TRAP mRNA expression with its activity. NFATc1 plays an essential role in the regulation of genes during the middle or late stages of osteoclast differentiation mediated by RANKL, and induces the expressions of osteoclast-specific genes, including OSCAR, TRAP, cathepsin K, and DC-STAMP [29–31]. Disruptions of the genes encoding these proteins were found to lead to osteopetrosis in mice [32,33]. Consistent with these reports, our results showed cotreatment with 10 μM cilostazol and 0.3 μM celecoxib synergistically inhibited RANKL-induced OSCAR, TRAP, DC-STAMP, and cathepsin K mRNA expressions by suppressing NFATc1, which indicated cooperation of NFATc1 with osteoclast-specific genes is indispensable for osteoclast differentiation, as was previously suggested by Takayanagi [28].

Furthermore, we confirmed that osteoclast formation by BMDMs obtained from C57BL/6 mice was markedly suppressed by cilostazol and celecoxib co-treatment. As was expected, osteoclast formation was strongly inhibited by cilostazol and celecoxib co-treatment. Interestingly, cilostazol and celecoxib co-treatment-induced down-regulations of NFATc1 protein and TRAP activity were reversed by IL-10 neutralizing antibody, these results indicating involvement of IL-10 in the down-regulation of osteoclast formation by cilostazol and celecoxib co-treatment.

Next, we examined whether cilostazol and celecoxib co-treatment inhibits the bone resorbing abilities of mature osteoclasts. It was reported that osteoclasts serve a crucial function in bone, possessing the unique ability to resorb bone matrix [30,31]. Fusion of mononuclear osteoclasts is essential for the formation of mature multinucleated osteoclasts, and osteoclast fusion by DC-STAMP is a primary regulator of bone resorption [34,35]. Cathepsin K is an osteoclast-specific lysosomal cysteine protease, is abundant in osteoclasts, and is required for the degradation of bone matrices and for bone resorption [33], which makes cathepsin K an important potential therapeutic targets for the treatment of bone diseases such as osteoporosis and autoimmune arthritis, in which osteoclast activity is increased [23].

As was reported by Song et al. [36], the exogeneous expression of NFATc1 in osteoclasts strongly induced pit and actin ring formation (important indicators of bone resorption). This suggests osteoclasts over-expressing NFATc1 can resorb bone and that NFATc1 inactivation might inhibit RANKL-induced bone resorption. In the present study, extensive pit formation observed in dentin slices in the BMDMs cultured in the presence of RANKL and M-CSF was markedly prevented by cilostazol and celecoxib co-treatment. Actin rings are produced by osteoclasts and are essential for bone resorption [37]. Therefore, the reductions in actin ring formation observed after cilostazol and celecoxib co-treatment indicate that these drugs affected the integrity of actin rings in osteoclasts, and thus, inhibited bone resorption.

Cilostazol was reported to induce IL-10 release from RA macrophages to medium, and to reduce LPS-induced increases in the productions of TNF-α and IL-1β [13]. Likewise, in our immunohistochemical study, elevated RANK and TNF-α expressions in the joints of vehicle-treated CIA mice were markedly diminished by cilostazol and celecoxib co-treatment, but only marginally reduced by either monotherapy. In line with these findings, serum IL-10 levels were markedly increased in mice cotreated with cilostazol and celecoxib, and serum IL-1β levels were significantly decreased, indicating that cilostazol and celecoxib co-treatment synergistically increased anti-inflammatory IL-10 and suppressed pro-inflammatory IL-1β.

Until present time, no current single medication has succeeded in healing destructive bone in RA. Generally, it appears single drugs require long-term therapy with high doses for effectiveness, and such treatments are likely to have serious side effects such as ulcer formation and upper gastrointestinal bleeding, impaired coagulation, cardiovascular effects and renal dysfunction [38]. Accordingly, multitarget-based drug combinations with lower doses may offer a possible means of developing more effective treatments with fewer side effects.

Taken together, it is concluded that cotreatment with cilostazol and celecoxib at lower doses than are normally prescribed will ensure a synergistic anti-arthritic potential for long-term treatment.

Declaration of Competing Interest

The authors declare no potential conflicts of interest.

Acknowledgments

This study was supported by the National Research Foundation of Korea (NRF-2016R1C1B2007691) and the Medical Research Center (MRC) Program through the National Research Foundation of Korea (NRF) grant funded by the Korea government (MSIP) (NRF-2015R1A5A2009656).

References

[1] A. Baier, I. Meineckel, S. Gay, T. Pap, Apoptosis in rheumatoid arthritis, Curr. Opin. Rheumatol. 15 (2003) 274–279.
[2] E.H. Choy, G.S. Panayi, Cytokine pathways and joint inflammation in rheumatoid arthritis, N. Engl. J. Med. 344 (2001) 907–916, https://doi.org/10.1056/NEJM200103223441207.
[3] I.B. McInnes, G. Schett, Cytokines in the pathogenesis of rheumatoid arthritis, Nat. Rev. Immunol. 7 (2007) 429–442, https://doi.org/10.1038/nri2094.
[4] Y. Wu, J. Liu, X. Feng, P. Yang, X. Xu, et al., Synovial fibroblasts promote osteoclast formation by RANKL in a novel model of spontaneous erosive arthritis, Arthritis Rheum. 52 (2005) 3257–3268, https://doi.org/10.1002/art.21354.
[5] H. Hsu, D.L. Lacey, C.R. Dunstan, I. Solovyev, A. Colombero, et al., Tumor necrosis factor receptor family member RANK mediates osteoclast differentiation and activation induced by osteoprotegerin ligand, Proc. Natl. Acad. Sci. U. S. A. 96 (1999) 3540–3545.
[6] H. Yasuda, N. Shima, N. Nakagawa, K. Yamaguchi, M. Kinosaki, et al., Osteoclast differentiation factor is a ligand for osteoprotegerin/osteoclastogenesis-inhibitory factor and is identical to TRANCE/RANKL, Proc. Natl. Acad. Sci. U. S. A. 95 (1998) 3597–3602.
[7] W.J. Boyle, W.S. Simonet, D.L. Lacey, Osteoclast differentiation and activation, Nature 423 (2003) 337–342, https://doi.org/10.1038/nature01658.
[8] S.L. Teitelbaum, F.P. Ross, Genetic regulation of osteoclast development and function, Nat. Rev. Genet. 4 (2003) 638–649, https://doi.org/10.1038/nrg1122.
[9] S.Y. Han, N.K. Lee, K.H. Kim, I.W. Jang, M. Yim, et al., Transcriptional induction of cyclooxygenase-2 in osteoclast precursors is involved in RANKL-induced

osteoclastogenesis, Blood 106 (2005) 1240–1245, https://doi.org/10.1182/blood-2004-12-4975.
[10] H.Y. Yoon, E.G. Lee, H. Lee, I.J. Cho, Y.J. Choi, et al., Kaempferol inhibits IL-1β-induced proliferation of RA SF and the production of COX-2, PGE2 and MMPs, Int. J. Mol. Med. 32 (2013) 971–977, https://doi.org/10.3892/ijmm.2013.1468.
[11] S.Y. Park, S.W. Lee, H.K. Shin, W.S. Lee, B.Y. Rhim, et al., Cilostazol inhibits proliferation and enhances apoptosis of synovial cells from patient with rheumatoid arthritis with suppression of inflammatory cytokine production via Nrf2- mediated heme oxygenase-1 induction, Arthritis Rheum. 62 (2010) 732–741, https://doi.org/10.1002/art.27291.
[12] S.Y. Park, H.Y. Kim, H.J. Park, H.K. Shin, K.W. Hong, et al., Concurrent treatment with taxifolin and cilostazol on the lowering of β-amyloid accumulation and neurotoxicity via the suppression of P-JAK2/P-STAT3/NF-κB/BACE1 signaling pathways, PLoS One 11 (2016) e0168286, , https://doi.org/10.1371/journal.pone.0168286.
[13] S.Y. Park, S.W. Lee, S.H. Baek, C.W. Lee, W.S. Lee, et al., Suppression of PU.1-linked TLR4 expression by cilostazol with decrease of cytokine production in macrophages from patients with rheumatoid arthritis, Br. J. Pharmacol. 168 (2013) 1401–1411, https://doi.org/10.1111/bph.12021.
[14] L.K. Myers, A.H. Kang, A.E. Postlethwaite, E.F. Rosloniec, S.G. Morham, et al., The genetic ablation of cyclooxygenase 2 prevents the development of autoimmune arthritis, Arthritis Rheum. 43 (2000) 2687–2693, https://doi.org/10.1002/1529-0131(200012) 43:12<2687:AID-ANR8>3.0.CO;2-9.
[15] S.M. Paulissen, J.P. van Hamburg, N. Davelaar, P.S. Asmawidjaja, J.M. Hazes, et al., Synovial fibroblasts directly induce Th17 pathogenicity via the cyclooxygenase/prostaglandin E2 pathway, independent of IL-23, J. Immunol. 191 (2013) 1364–1372, https://doi.org/10.4049/jimmunol.1300274.
[16] M. Funakoshi-Tago, T. Shimizu, K. Tago, M. Nakamura, H. Itoh, et al., Celecoxib potently inhibits TNFα-induced nuclear translocation and activation of NF-κB, Biochem. Pharmacol. 76 (2008) 662–671, https://doi.org/10.1016/j.bcp.2008.06.015.
[17] R.O. Williams, M. Feldmann, R.N. Maini, Anti-tumor necrosis factor ameliorates joint disease in murine collagen-induced arthritis, Proc. Natl. Acad. Sci. U. S. A. 89 (1992) 9784–9788.
[18] S.Y. Park, S.W. Lee, H.Y. Kim, S.Y. Lee, W.S. Lee, et al., SIRT1 inhibits differentiation of monocytes to macrophages: amelioration of synovial inflammation in rheumatoid arthritis, J. Mol. Med. (Berl) 94 (2016) 921–931, https://doi.org/10.1007/s00109-016-1402-7.
[19] S.L. Teitelbaum, Bone resorption by osteoclasts, Science 289 (2000) 1504–1508.
[20] H. Huang, J. Ryu, J. Ha, E.J. Chang, H.J. Kim, et al., Osteoclast differentiation requires TAK1 and MKK6 for NFATc1 induction and NF-κB transactivation by RANKL, Cell Death Differ. 13 (2006) 1879–1891, https://doi.org/10.1038/sj.cdd.4401882.
[21] H.Y. Kim, S.W. Lee, S.Y. Park, S.H. Baek, C.W. Lee, et al., Efficacy of concurrent administration of cilostazol and methotrexate in rheumatoid arthritis: pharmacologic and clinical significance, Life Sci. 91 (2012) 250–257, https://doi.org/10.1016/j.lfs.2012.07.003.
[22] P. Isomaki, R. Luukkainen, R. Saario, P. Toivanen, J. Punnonen, Interleukin-10 functions as an antiinflammatory cytokine in rheumatoid synovium, Arthritis Rheum. 39 (1996) 386–395.
[23] H. Takayanagi, Osteoimmunology: shared mechanisms and crosstalk between the immune and bone systems, Nat. Rev. Immunol. 7 (2007) 292–304, https://doi.org/10.1038/nri2062.
[24] Z.H. Lee, H.H. Kim, Signal transduction by receptor activator of nuclear factor kappa B in osteoclasts, Biochem. Biophys. Res. Commun. 305 (2003) 211–214.
[25] T. Yamashita, Z. Yao, F. Li, Q. Zhang, I.R. Badell, et al., NF-κB p50 and p52 regulate receptor activator of NF-κB ligand (RANKL) and tumor necrosis factor-induced osteoclast precursor differentiation by activating c-Fos and NFATc1, J. Biol. Chem. 282 (2007) 18245–18253, https://doi.org/10.1074/jbc.M610701200.
[26] K.A. Mensah, C.T. Ritchlin, E.M. Schwarz, RANKL induces heterogeneous DCSTAMP (lo) and DC-STAMP (hi) osteoclast precursors of which the DCSTAMP (lo) precursors are the master fusogens, J. Cell. Physiol. 223 (2010) 76–83, https://doi.org/10.1002/jcp.22012.
[27] C. Zhang, C.E. Dou, J. Xu, S. Dong, DC-STAMP, the key fusion-mediating molecule in osteoclastogenesis, J. Cell. Physiol. 229 (2014) 1330–1335 https://doi.org/10.1002/jcp.24553.
[28] H. Takayanagi, Mechanistic insight into osteoclast differentiation in osteoimmunology, J. Mol. Med. (Berl). 83 (2005) 170–179, https://doi.org/10.1007/s00109-004-0612-6.
[29] N. Kim, M. Takami, J. Rho, R. Josien, Y. Choi, A novel member of the leukocyte receptor complex regulates osteoclast differentiation, J. Exp. Med. 195 (2002) 201–209.
[30] K. Kim, J.H. Kim, J. Lee, H.M. Jin, S.H. Lee, et al., Nuclear factor of activated T cells c1 induces osteoclast-associated receptor gene expression during tumor necrosis factor-related activation-induced cytokine-mediated osteoclastogenesis, J. Biol. Chem. 280 (2005) 35209–35216, https://doi.org/10.1074/jbc.M505815200.
[31] Y. Kim, K. Sato, M. Asagiri, I. Morita, K. Soma, et al., Contribution of nuclear factor of activated T cells c1 to the transcriptional control of immunoreceptor osteoclast-associated receptor but not triggering receptor expressed by myeloid cells-2 during osteoclastogenesis, J. Biol. Chem. 280 (2005) 32905–32913, https://doi.org/10.1074/jbc.M505820200.
[32] A.R. Hayman, S.J. Jones, A. Boyde, D. Foster, W.H. Colledge, et al., Mice lacking tartrate-resistant acid phosphatase (Acp 5) have disrupted endochondral ossification and mild osteopetrosis, Development 122 (1996) 3151–3162.
[33] P. Saftig, E. Hunziker, O. Wehmeyer, S. Jones, A. Boyde, et al., Proc. Natl. Acad. Sci. U. S. A. 95 (1998) 13453–13458.
[34] H. Miyamoto, T. Suzuki, Y. Miyauchi, R. Iwasaki, T. Kobayashi, et al., Osteoclast stimulatory transmembrane protein and dendritic cell specific transmembrane protein cooperatively modulate cell-cell fusion to form osteoclasts and foreign body giant cells, J. Bone Miner. Res. 27 (2012) 1289–1297, https://doi.org/10.1002/jbmr.1575.
[35] M. Yagi, T. Miyamoto, Y. Sawatani, K. Iwamoto, N. Hosogane, et al., DC-STAMP is essential for cell-cell fusion in osteoclasts and foreign body giant cells, J. Exp. Med. 202 (2005) 345–351, https://doi.org/10.1084/jem.20050645.
[36] I. Song, J.H. Kim, K. Kim, H.M. Jin, B.U. Youn, et al., Regulatory mechanism of NFATc1 in RANKL-induced osteoclast activation, FEBS Lett. 583 (2009) 2435–2440, https://doi.org/10.1016/j.febslet.2009.06.047.
[37] T. Suda, I. Nakamura, E. Jimi, N. Takahashi, Regulation of osteoclast function, J. Bone Miner. Res. 12 (1997) 869–879, https://doi.org/10.1359/jbmr.1997.12.6.869.
[38] M.L. Capone, S. Tacconelli, L.G. Rodriguez, P. Patrignani, NSAIDs and cardiovascular disease: transducing human pharmacology results into clinical read-outs in the general population, Pharmacol. Rep. 62 (2010) 530–535 (PMID: 20631418).